

Binding of nucleic acids to *E.coli* RNase HI observed by NMR and CD spectroscopy

Yasushi Oda, Shigenori Iwai¹, Eiko Ohtsuka¹, Momoyo Ishikawa, Morio Ikehara and Haruki Nakamura*

Protein Engineering Research Institute, Furuedai, Suita, Osaka 565 and ¹Faculty of Pharmaceutical Sciences, Hokkaido University, Sapporo 060, Japan

Received July 15, 1993; Revised and Accepted September 1, 1993

ABSTRACT

To clarify the mechanism by which the RNA portion of a DNA/RNA hybrid is specifically hydrolyzed by ribonuclease H (RNase H), the binding of a DNA/RNA hybrid, a DNA/DNA duplex, or an RNA/RNA duplex to RNase HI from *Escherichia coli* was investigated by ¹H-¹⁵N heteronuclear NMR. Chemical shift changes of backbone amide resonances were monitored while the substrate, a hybrid 9-mer duplex, a DNA/DNA 12-mer duplex, or an RNA/RNA 12-mer duplex was titrated. The amino acid residues affected by the addition of each 12-mer duplex were almost identical to those affected by the substrate hybrid binding, and resided close to the active site of the enzyme. The results reveal that all the duplexes, hybrid-, DNA-, and RNA-duplex, bind to the enzyme. From the linewidth analysis of the resonance peaks, it was found that the exchange rates for the binding were different between the hybrid and the other duplexes. The NMR and CD data suggest that conformational changes occur in the enzyme and the hybrid duplex upon binding.

INTRODUCTION

Ribonuclease H (RNase H) is a unique endo-ribonuclease that specifically cleaves the RNA strand of a DNA/RNA hybrid, yielding a 3'-hydroxyl and a 5'-phosphate at the hydrolysis site (1). This enzyme requires specific divalent cations, such as Mg²⁺ or Mn²⁺, for its enzymatic activity.

The enzyme is widely present in various organisms (1), including retroviruses as a domain of the reverse transcriptase (2). The three-dimensional structure of the RNase H domain in human immunodeficiency virus-1 (HIV-1) (3–5) is similar to that of *Escherichia coli* (*E.coli*) RNase HI (6–8) and *Thermus thermophilus* RNase H (9). The physiological function of RNase H remains obscure, although biological studies suggest that it is associated with DNA replication and repair in the cell (10), or with reverse-transcription in retroviruses (2).

From a series of site directed mutagenesis experiments (11) and a computer analysis of RNase H amino acid sequences (12), the catalytic residues of *E.coli* RNase HI were determined to be

Asp10, Glu48, and Asp70. It has been confirmed by X-ray crystallographic and NMR studies that these three residues form an active site in the enzyme (6–8), and that Mg²⁺ (6,7,13) and the substrate DNA/RNA hybrid (14) bind close to this region.

A model complex has been built based on the free structures of the enzyme and the substrate independently determined by X-ray crystallography and NMR distance geometry, respectively (14). In the modeling of the complex, we assumed that the hybrid adopts an A-form double-helical conformation. This assumption was based on the structural analysis of a chimeric DNA/RNA hybrid, (GmUmCm-dAdTdCdT-CmCm)/r(GGAGAUGAC) (designated as hybrid 9-mer). The chimeric DNA contains four successive deoxyribonucleotides among 2'-O-methylnucleotides in the DNA strand. RNase H has only a slight specificity for the base sequence of the hybrid. However, using the chimeric DNA as a complementary strand to RNA, the RNA strand can be cleaved at a specific position (15). So, we chose the chimeric hybrid in the previous NMR study to investigate the specific interactions. It should be noted that a tetranucleotide duplex is considered to be the minimum unit of substrate hybrids recognized by the enzyme (15,16).

The model structure of the substrate–enzyme complex is constructed by considering the three structural bases: (i) the steric complement between the molecular surfaces of the enzyme and the hybrid double helix—that is, the interface of the enzyme has a shape looping around the double helical structure; (ii) the electrostatic complement between them—that is, the interface of the enzyme has a positively charged cluster interacting with the negatively charged nucleic acids; and (iii) the special interactions between functional groups of the enzyme and the substrate, which were confirmed by site-directed mutagenesis. Similar assumptions were made in modeling the complex (5,8).

In the present study, we focus on the interactions of (i) and (ii), which seem to be global and nonspecific. If the steric and electrostatic complements are important factors for the global recognition, DNA/DNA or RNA/RNA duplexes, which are not cleaved by RNase H, should bind to the enzyme because they assume double helical structures like the DNA/RNA hybrid. Therefore, we also examined the binding of DNA/DNA and RNA/RNA duplexes to RNase H.

* To whom correspondence should be addressed

It is well known that nucleic acid duplexes assume two typical helical structures, the A- and B-forms; DNA duplexes are generally in a B-form, and RNA duplexes are in an A-form structure (17). We focused on the binding of these two type of duplexes to the enzyme. For the DNA duplex, we chose a synthetic self-complementary 12-mer, d(CGCGAATTCGCG) (designated DNA 12-mer), the duplex of which assumes the B-form both in crystal (18) and solution (19,20). For the RNA duplex, we chose a synthetic self-complementary 12-mer, r(CGCGAAUUCGCG) (designated RNA 12-mer), the duplex of which assumes an A-form in solution (21).

The conformational change of the DNA/RNA hybrid was examined upon binding to RNase H. We performed the experiment using circular dichroism (CD) spectroscopy, because of problems with the solubility of the complex. In the titration experiment, we chose a synthetic oligonucleotide duplex, d(GTCATCTCCAG)/r(CUGGAGAUGAC) (designated hybrid 11-mer), and a longer duplex, d(GTCATCTCCAGGTCATCTCCAG)/r(CUGGAGAUGAC)·r(CUGGAGAUGAC) (designated hybrid 22-mer). These hybrids include the same base sequence of the above chimeric hybrid 9-mer. The hybrid 22-mer duplex is a repeated sequence of the hybrid 11-mer, and is nicked in the center of the RNA strand because of the synthesis method. This duplex has a length sufficient to cover the whole binding interface of the enzyme, as estimated from the model building.

MATERIALS AND METHODS

Sample preparation

The preparation and purification of *E. coli* RNase HI was as described previously (14). To uniformly label the enzyme with ¹⁵N, *E. coli* strain JM109, in which plasmid pJAL600 (22) was cloned, was grown in M9 minimum culture medium, including 1g/liter culture of [¹⁵N]-NH₄Cl (99.8 atom%, Shoko Co. Ltd., Tokyo).

The deoxyribonucleotide 11-mer, d(GTCATCTCCAG) (DNA 11-mer), the deoxyribonucleotide 22-mer, d(GTCATCTCCAGGTCATCTCCAG) (DNA 22-mer), and the self-complementary deoxyribonucleotide 12-mer, d(CGCGAATTCGCG) (DNA 12-mer), were synthesized chemically on an automated synthesizer (Applied Biosystems Model 380B). The chimeric nucleotide 9-mer, (GmUmCm-dAdTdCdT-CmCm) (chimera 9-mer), was synthesized chemically following the procedure of (15). The ribonucleotide 9-mer, r(GGAGAUGAC) (RNA 9-mer), the ribonucleotide 11-mer, r(CUGGAGAUGAC) (RNA 11-mer), the ribonucleotide 3-mer, r(AAU) (RNA 3-mer), and the self-complementary ribonucleotide 12-mer, r(CGCGAAUUCGCG) (RNA 12-mer), were synthesized chemically following the procedure of (23). Each of the purified oligonucleotides was desalted by gel filtration on Sephadex G-10 (except for RNA 3-mer), and was converted to the sodium salt by an ion exchange column. The hybrid 9-mer duplex was prepared by mixing equi-molar amounts of the chimera 9-mer and the RNA 9-mer. The hybrid 11-mer duplex was prepared by mixing equi-molar amounts of the DNA 11-mer and the RNA 11-mer. The hybrid 22-mer duplex was prepared by combining the DNA 22-mer and the RNA 11-mer at a molar ratio of 1:2.

Titration experiment using NMR spectroscopy

Chemical shift changes of the backbone amide ¹H and ¹⁵N resonances of the uniformly ¹⁵N-labeled enzyme during the titration with each of the nucleic acids and KCl were observed

using a ¹H-¹⁵N heteronuclear two dimensional (2D) NMR technique, ¹H-¹⁵N heteronuclear single-quantum coherence (HSQC) spectroscopy (24), as previously reported for the hybrid 9-mer (14). All the titration measurements were performed at 27°C.

For the titration of the oligonucleotide duplexes, the enzyme and each of the duplexes were dissolved in 10 mM sodium acetate (pH 5.5) with 0.3 M KCl and 0.1 mM EDTA in 90% H₂O/10% D₂O. The concentration of the enzyme was 1.1 mM, that of the hybrid 9-mer duplex was 3.3 mM, and those of the DNA and RNA 12-mers were 3.0 mM. In the course of the titration, 5–50 μl oligonucleotide solution was added to 270–280 μl enzyme solution. Molar ratios of the oligonucleotide duplex to the enzyme were 0, 0.05, 0.1, 0.2, 0.3, and 0.5 (0.4 for the DNA and RNA 12-mers). The chemical shift changes upon the addition of 0.3 M KCl were monitored by comparing the spectra of the enzyme solution in the absence and presence of KCl. For the titration of the RNA 3-mer, the enzyme and the RNA 3-mer were dissolved in 0.1 M sodium acetate (pH 5.5) with 0.1 M MgCl₂ in 90% H₂O/10% D₂O. This concentration of MgCl₂ is a saturated condition for Mg²⁺ ion binding to the active site of the enzyme (13). The concentrations of the enzyme and the RNA 3-mer were 1 mM and 73 mM, respectively. During the course of titration, 0.5–25 μl oligonucleotide solution was added to 300 μl enzyme solution. Molar ratios of the oligonucleotide to the enzyme were 0, 0.1, 0.5, 1, 2, and 5.

All the NMR spectra were measured on a 500 MHz (for ¹H) spectrometer (Bruker AM-500). We used the pulse sequence of HSQC proposed by Bax and colleagues (25). The resonance of residual H₂O was suppressed by preirradiation. The 2D NMR spectra were acquired with 512 increments in the t₁ direction, and 2048 data points in the t₂ direction. The time domain data were multiplied by a phase shift sine bell squared window function in both the t₁ and t₂ directions, and zero-filled to 2048 in the t₁ dimension and to 4096 in the t₂ dimension before Fourier transformation. The spectral width of ω₁ (¹⁵N resonances) was 2315 Hz and that of ω₂ (¹H resonances) was 7042 Hz. ¹H chemical shifts are relative to the water signal (4.78 ppm relative to sodium 3-(trimethylsilyl)propionate). ¹⁵N chemical shifts are relative to the ¹⁵N signal of formamide (113.3 ppm).

Titration experiment using CD spectroscopy

CD spectra were recorded on a J-600 spectropolarimeter (Japan Spectroscopic) with an 10-mm path-length cuvette. The enzyme and each of the hybrid duplexes were dissolved in 10 mM Tris·HCl (pH 7.5) with 1 mM EDTA. The concentrations of the hybrid 11-mer and the 22-mer duplex were 4.09 μM and 2.31 μM, respectively, and that of the enzyme was 0.51 mM. In the course of titration, 1–40 μl enzyme solution was added to 2 ml oligonucleotide solution. Molar ratios of the enzyme to the hybrid duplex were 0, 0.1, 0.2, 0.5, 1, 2, 4, and 5. The titration measurements were performed at 25°C.

RESULTS AND DISCUSSION

Binding of A- and B-form double helices to RNase H

To examine the binding of the nucleic acid duplexes to *E. coli* RNase HI, we performed titrations of the uniformly ¹⁵N-labeled enzyme with the RNA or DNA 12-mer duplexes using a ¹H-¹⁵N heteronuclear two dimensional (2D) NMR technique, HSQC experiment. Figure 1 shows the expanded HSQC spectra of the enzyme in a cross-peak region of the backbone amide ¹H and

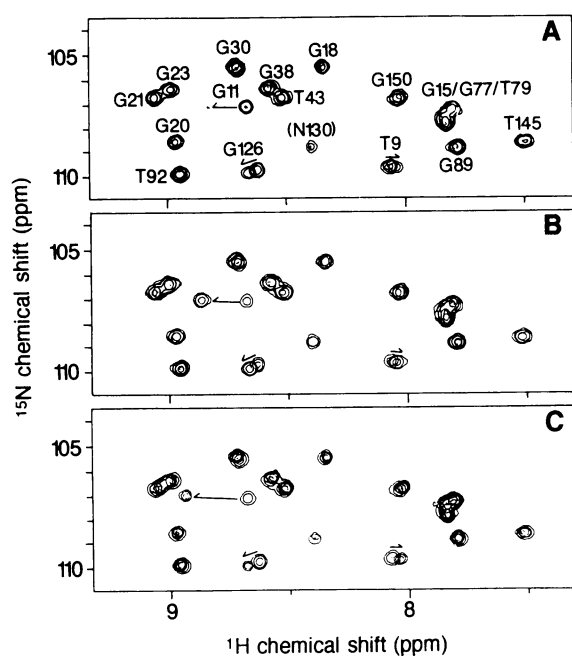


Figure 1. Expanded ^1H - ^{15}N HSQC spectra in a backbone amide region of uniformly ^{15}N -labeled *E. coli* RNase HI in H_2O - D_2O (9:1) containing 0.3 M KCl, 0.1 mM EDTA, and 10 mM sodium acetate buffer (pH 5.5) at 27°C . The spectrum of the free-enzyme is superimposed on each spectrum in the presence (0.3 eq. molar) of hybrid 9-mer (A), RNA 12-mer (B), and DNA 12-mer (C). Peak assignments are indicated in the panel (A). Arrows indicate the direction of the peak shift following the nucleic acid binding.

^{15}N resonances. Chemical shift changes of several backbone amide peaks were observed upon the titrations with both the RNA and DNA 12-mers, as reported for the hybrid 9-mer duplex (14). This result indicates that all of the duplexes bind to the enzyme.

The chemical shifts of the backbone amide peaks have been completely assigned to the corresponding residues (26). Therefore, the amino acid residues responsible for the nucleic acid binding could be mapped. Figure 2 shows the chemical shift change ($\Delta\delta$) of the backbone amide ^1H and ^{15}N resonances in the titrations with hybrid 9-mer, DNA 12-mer, or RNA 12-mer at the molar ratio of 0.3. The residues engaged in the binding of the duplexes are clearly identified. The affected residues are almost identical among the three duplexes, indicating that all of the duplexes bind to the same site of the enzyme.

The chemical shift changes by the addition of KCl were also examined. The distribution of the affected residues with KCl is clearly different from that with the nucleic acid duplexes (Fig. 3); for example, the residues within the N-terminal loop and the loop between βB and βC are affected. They form the other positive charged cluster of the enzyme than the binding interface of the nucleic acid duplexes. This implies that the nucleic acid duplexes bind to a specific site.

The residues affected by the duplexes reside close to the active site, especially around the catalytic residues of Asp10 and Asp70. The site around His83 and Asn84 is also affected by duplex binding. This may be due to an ionization-state change of the imidazole ring of His83, as mentioned (14). On the other hand, His83 and Asn84 are located in the N-terminal portion of the αIII helix, beside the joint connecting the αII and αIII helices, and their backbone amides are not involved in hydrogen bonds

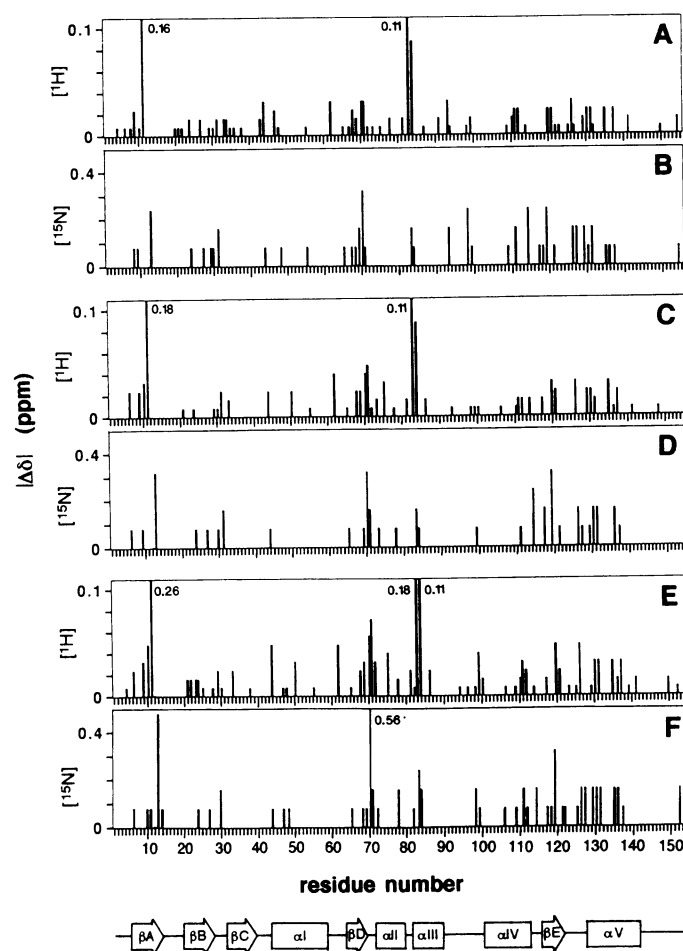


Figure 2. The absolute backbone amide chemical shift changes ($|\Delta\delta|$) between the absence and presence (0.3 eq. molar) of hybrid 9-mer in the ^1H axis (A), in the ^{15}N axis (B), RNA 12-mer in the ^1H axis (C), in the ^{15}N axis (D), DNA 12-mer in the ^1H axis (E), and in the ^{15}N axis (F). The following residues, for which peak assignments were ambiguous because of peak overlapping in the course of titration, are omitted from the analysis: V5, I7, S12, G15, N16, E32, T40, N45, R46, L49, I53, V54, L56, E57, K60, C63, E64, V74, Q76, G77, T79, Q80, W85, R88, W104, L107, D108, Q113, Q115, H124, C133, D134, R138, E147, T149, and V153. The elements of regular secondary structure are shown below the diagram. The amino-acid sequence of the enzyme is published (6,11).

(7). The observed changes for His83 and Asn84 suggest a conformational change in the vicinity of the joint to adjust the steric or electrostatic complement of the binding surface. The relationship between the conformation of the joint and the activity has also been revealed by the X-ray analysis of *Thermus thermophilus* RNase H, in which the joint site is stabilized by additional hydrogen bonds (9). Chemical shift changes are also observed in the region between βE and αV . This region is joined by a loop containing the well conserved residues, His124 and Asn130. It has been reported that His124 is involved in the catalytic function of the enzyme (27). The observed chemical shift changes suggest a conformational change in this region following the nucleic acid binding. It has been pointed out that the conformation of the loop is rather flexible, and that the flexibility around this loop is important for the enzymatic activity (9,27,28). The present result supports this proposal.

It should be noted that the chemical shift change seems to be generally larger for the amide that is not involved in a hydrogen

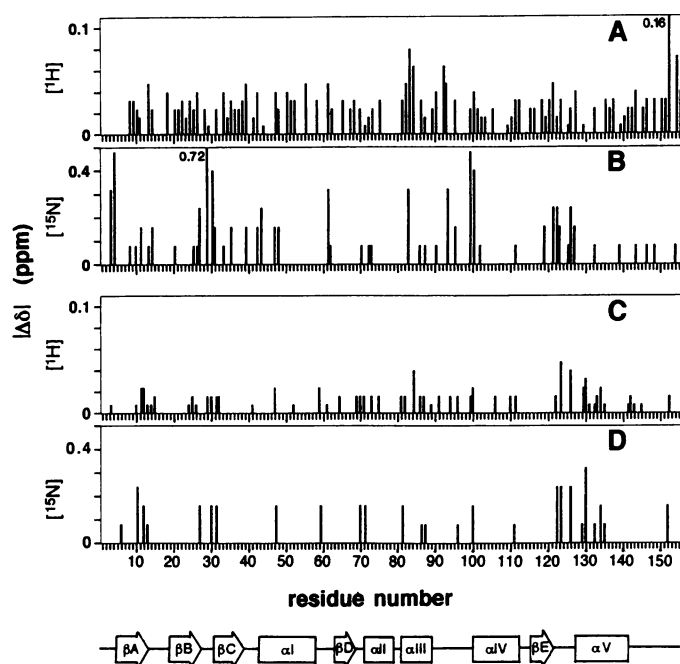


Figure 3. The absolute backbone amide chemical shift changes ($\Delta\delta$) between the absence and presence of KCl (0.3 M) in the ^1H axis (A), in the ^{15}N axis (B), RNA 3-mer (5 eq. molar) in the ^1H axis (C), and in the ^{15}N axis (D). The omitted residues from the analysis for KCl are the same as in Fig. 2, and for the RNA 3-mer are as follows: L2, Q4, V5, N16, L49, V54, L56, H62, V65, V74, Q80, H83, R88, A93, W104, Q113, H114, Q115, H124, H127, A137, R138, A139, and V153. The difference in the omitted residues between the RNA 3-mer and the others is due to the different solvent conditions in the experiments.

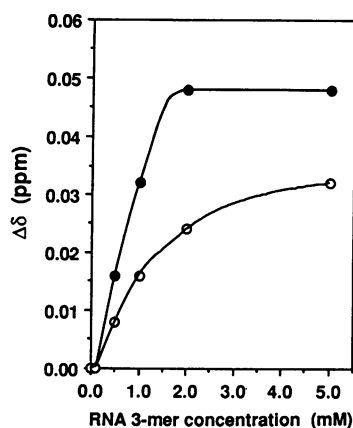


Figure 4. Titration curves of the RNA 3-mer binding to *E. coli* RNase HI, obtained from the ^1H chemical-shift changes for Gly123 (closed circle) and Gly126 (open circle) in the course of the titration with the enzyme. The data for Gly126 were analyzed by Hill plot to calculate the dissociation constant of the RNA 3-mer. The $\Delta\delta$ value in the presence of 5 mM RNA 3-mer was considered to be the maximal change for the analysis.

bond. Therefore, the magnitude of the chemical shift change does not always correspond to that of the conformational change.

The clear difference between the substrate hybrid and the other duplexes in the experiments was observed in the linewidth of the resonance peaks. Significant broadening occurred in several peaks upon the titration with the substrate hybrid, but not with the DNA

and RNA duplexes; for example, Gly11 in Fig. 1. This suggests that the exchange rate between the free- and bound-forms (dissociation rate) is different; the exchange rate of residues, whose resonance peaks are broadened, are slower than the others. It may be due to a different rate of the local conformational change of each residue following the substrate binding. Another possibility for the cause of the broadening should be considered; the increase of the exchange rate between the labile amide proton and the solvent H_2O , which occurs as a result of the increase in the local pH around the amide group following the tight binding of the substrate.

We also examined the binding of a short single-strand oligonucleotide, an RNA 3-mer, to the Mg^{2+} -bound enzyme. The active site of the enzyme forms a negatively charged cluster (6,8). Therefore, it seems that the interactions of negatively charged nucleic acids with the active site would be repulsive. It is expected that the Mg^{2+} binding to the active site weakens the repulsive charged effect between them. The distribution of the affected residues with the RNA 3-mer is different from those with the duplexes (Fig. 3). Figure 4 shows the ^1H chemical-shift changes of Gly123 and Gly126 during the titration with the RNA 3-mer. From the Hill plot analysis of the data for Gly126, the dissociation constant, K_D , and the number of bound oligomers per enzyme, n , were calculated to be 2×10^{-5} M and 1.6, respectively. Taking into account the quality of the experimental data, it is estimated that the RNA 3-mer has a K_D value above 10^{-5} M. This result shows that the short RNA 3-mer binding is fairly weak, as compared to the substrate-hybrid binding ($K_D = 10^{-8} - 10^{-9}$ M) described below. The results for the RNA 3-mer support the consideration in the model building that a considerably longer double helical structure would be required for the formation of the complex.

Electrostatic interaction in the binding

In the course of titration with the hybrid 9-mer, a large amount of precipitate appeared when the molar ratio of the hybrid to the enzyme exceeded 0.3, and the NMR signal became too weak to observe cross peaks because of the decrease in the soluble protein concentration. The precipitate was tested to determine whether it contained the hybrid 9-mer. The precipitate was dissolved in a sufficient amount of water containing 0.3 M KCl, and was analyzed by ion-exchange column chromatography. The HPLC pattern of the heated solution at 60°C revealed that both strands of the hybrid 9-mer are contained in the precipitate, showing that the precipitate is a complex of the enzyme and the hybrid duplex.

It is known that protein-DNA binding interactions are highly dependent upon salt concentrations, with the general observation that binding affinities decrease with increasing salt concentration, because of the shielding of electrostatic interactions between them (29). In the case of *E. coli* RNase HI, when the titration experiments were performed in the solution without KCl, much more precipitate appeared. The amount of the precipitate decreased with increasing KCl concentration, suggesting that the electrostatic interactions between the enzyme and the hybrid duplex are weakened by the added salt, KCl.

Precipitation was also observed in the titrations for the other duplexes. Therefore, it is difficult to obtain the binding constant of each duplex to the enzyme. The observed amount of precipitated complex was DNA/RNA \gg RNA/RNA $>$ DNA/DNA. If the amount of precipitate is assumed to reflect the strength of each duplex binding, especially by electrostatic interaction, then the substrate duplex is considered to interact

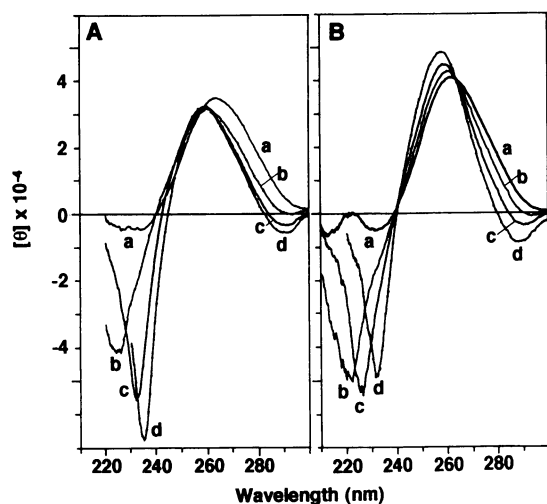


Figure 5. CD spectra of the hybrids in 10 mM Tris·HCl (pH 7.5) and 1 mM EDTA at 25°C; (A) hybrid 11-mer (a), and with the enzyme at 0.5 eq. (b), 2 eq. (c), and 5 eq. molar (d); (B) hybrid 22-mer (a), and with the enzyme at 1 eq. (b), 2 eq. (c), and 4 eq. molar (d).

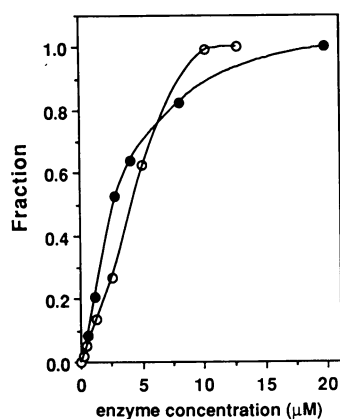


Figure 6. Titration curves of the enzyme binding to the hybrid 11-mer (closed circle) and the hybrid 22-mer (open circle). The data were obtained from the $[\theta]$ at 280 nm in the CD spectra of the hybrids. The fraction of the enzyme binding values were obtained from the $\Delta[\theta]/\Delta[\theta]_{\max.}$, which are the values of the $[\theta]$ change against the maximal $[\theta]$ change in the presence of 5 equi-molar enzyme.

with the enzyme much more tightly than the other duplexes. This is consistent with the above result for the line-broadening. The specific discrimination of the DNA/RNA hybrid for the enzyme catalysis may be achieved by the additional interactions that are classified in the interaction (iii) described above. It is thought that specific interactions through the 2'-OH are lacking in the DNA/DNA duplex, and several interactions are inhibited by steric hindrance between the enzyme and the additional 2'-OH of the strand opposite to the cleaved RNA strand in the RNA/RNA duplex.

Conformational changes upon the binding

The NMR data suggest that the conformation of the enzyme is altered (by induced fit) by the substrate binding, as discussed above. Although NMR spectroscopy will also be useful for structural analysis of the substrate hybrid in the complex, a

detailed analysis of the hybrid was difficult because of the low solubility (the precipitation) of the complex, as described above. Therefore, we performed the titration experiment while monitoring by CD spectroscopy to examine the conformational changes of the hybrid duplex upon binding.

Figure 5 shows the CD spectra of the hybrid 11-mer and 22-mer molecules. The CD spectra of both hybrids are typical of an A-form duplex. Following the binding of the enzyme, the maximum is blue-shifted from 263 nm to 258 nm, and a new minimum at 288 nm appears for both of the hybrids. The CD spectra of the bound-forms are essentially the same with the hybrid 11-mer and 22-mer, while the peak intensities at 258 nm are different for each of the hybrids. The spectral change observed in the 210–240 nm range is not considered at present, because a large negative molar ellipticity of the enzyme is overlapped in this region. Figure 6 shows the titration curves of the hybrids obtained from the CD data at 280 nm. From the Hill plot analyses of the CD data at 280 nm, the dissociation constant, K_D , and the numbers of bound duplexes per enzyme, n , were calculated as follows: $K_D = 5 \times 10^{-9}$ M and $n = 1.5$ for the hybrid 11-mer, and $K_D = 2 \times 10^{-8}$ M and $n = 1.4$ for the hybrid 22-mer. Taking the K_D values calculated from the data of the other wavelengths into consideration, the dissociation constants of the hybrids are evaluated in the range of 10^{-8} – 10^{-9} M in the solution containing 10 mM Tris·HCl (pH 7.5) with 1 mM EDTA at 25°C.

The CD data clearly show that the conformation of the hybrid duplex is altered by enzyme binding, and especially by an alteration in the base stacking. Previously, we proposed that the substrate hybrid should be bent (kinked) in the complex for exact fitting (14), as observed for several nucleases, such as DNase I (30) and *EcoRI* (31). The altered CD spectra of the hybrids suggest bending of the duplexes. It is also possible that the global helical conformation of the hybrid is altered from the A-form following the binding.

There are many publications describing the tertiary structures of DNA/RNA hybrids as determined by NMR (32–34), Raman spectroscopy (35), X-ray fiber diffraction (36,37), and X-ray crystallography (38). The results are often in disagreement with each other, and it should be considered that hybrids can have an A-form, B-form, or heterogeneous form (DNA strands with B-form and RNA strands with A-form) depending on the solvent conditions and the base sequences. Recently, Salazar *et al.* reported an interesting result determined by NMR, that the DNA strand in a DNA/RNA hybrid is neither B-form nor A-form, but an intermediate form (*O4'-endo*) in solution (39). The present results show that both A-form and B-form duplexes bind to RNase H, and that the structure of the hybrid duplex is altered in the substrate–enzyme complex. Therefore, to reveal the mechanism by which the RNA portion of the DNA/RNA hybrid is specifically hydrolyzed by RNase H, we should focus on the substrate structure in the complex. However, structural study of the hybrid will still provide important information about the mechanism. For example, Salazar *et al.* pointed out in their NMR study that the RNA strand has a longer T_1 relaxation time than the DNA strand in the hybrid (39). This agrees with the proposal that the flexibility of the strand opposite to the cleaved RNA strand is important for the specific recognition of RNase H (14).

ACKNOWLEDGEMENTS

The authors wish to thank Drs K.Morikawa, K.Katayanagi, K.Ishikawa, and S.Kanaya for discussions.

REFERENCES

1. Crouch, R. J. and Dirksen, M.-L. (1982) in *Nuclease* (Linn, S. M. and Roberts, R. J., Eds.) pp. 211–241, Cold Spring Harbor Laboratory, Cold Spring Harbor, New York.
2. Wintersberger, U. (1990) *Pharmac. Ther.* **48**, 259–280.
3. Davies, J. F., II, Hostomska, Z., Hostomsky, Z., Jordan, S. R. and Matthews, D. (1991) *Science* **252**, 88–95.
4. Arnold, E., Jacobo-Molina, A., Nanni, R. G., Williams, R. L., Lu, X., Ding, J., Clark Jr., A. D., Zhang, A., Ferris, A. L., Clark, P., Hizi, A. and Hughes, S. H. (1992) *Nature* **357**, 85–89.
5. Kohlstaedt, L. A., Wang, J., Friedman, J. M., Rice, P. A. and Steitz, T. A. (1992) *Science* **256**, 1783–1790.
6. Katayanagi, K., Miyagawa, M., Matsushima, M., Ishikawa, M., Kanaya, S., Ikehara, M., Matsuzaki, T. and Morikawa, K. (1990) *Nature* **347**, 306–309.
7. Katayanagi, K., Miyagawa, M., Matsushima, M., Ishikawa, M., Kanaya, S., Nakamura, H., Ikehara, M., Matsuzaki, T. and Morikawa, K. (1992) *J. Mol. Biol.* **223**, 1029–1052.
8. Yang, W., Hendrickson, W. A., Crouch, R. J. and Satow, Y. (1990) *Science* **249**, 1398–1405.
9. Ishikawa, K., Okumura, M., Katayanagi, K., Kimura, S., Kanaya, S., Nakamura, H. and Morikawa, K. (1993) *J. Mol. Biol.* **230**, 529–542.
10. Crouch, R. J. (1990) *The New Biologist* **2**, 771–777.
11. Kanaya, S., Kohara, A., Miura, Y., Sekiguchi, A., Iwai, S., Inoue, H., Ohtsuka, E. and Ikehara, M. (1990) *J. Biol. Chem.*, **265**, 4615–4621.
12. Doolittle, R. F., Feng, D.-F., Johnson, M. S. and McClure, M. A. (1989) *Quart. Rev. Biol.* **64**, 1–30.
13. Oda, Y., Nakamura, H., Kanaya, S. and Ikehara, M. (1991) *J. Biomolec. NMR* **1**, 247–255.
14. Nakamura, H., Oda, Y., Iwai, S., Inoue, H., Ohtsuka, E., Kanaya, S., Kimura, S., Katsuda, C., Katayanagi, K., Morikawa, K., Miyashiro, H. and Ikehara, M. (1991) *Proc. Natl. Acad. Sci. U.S.A.* **88**, 11535–11539.
15. Inoue, H., Hayase, Y., Iwai, S. and Ohtsuka, E. (1987) *FEBS Lett.* **215**, 327–330.
16. Donis-Keller, H. (1979) *Nucleic Acids Res.* **7**, 179–192.
17. Saenger, W. (1984) in *Principles of Nucleic Acid Structure* (Cantor, C. R., Ed.) pp. 220–282, Springer-Verlag, New York.
18. Dickerson, R. E. and Drew, H. R. (1981) *J. Mol. Biol.* **149**, 761–786.
19. Patel, D. J., Kozlowski, S. A., Marky, L. A., Broka, C., Rice, J. A., Itakura, K. and Breslauer, K. J. (1982) *Biochemistry* **21**, 428–436.
20. Hare, D. R., Wemmer, D. E., Chou, S.-H., Drobny, G. and Reid, B. R. (1983) *J. Mol. Biol.* **171**, 319–336.
21. Chou, S.-H., Flynn, P. and Reid, B. R. (1989) *Biochemistry* **28**, 2422–2435.
22. Kanaya, S., Oobatake, M., Nakamura, H. and Ikehara, M. (1993) *J. Biotechnology* **28**, 117–136.
23. Iwai, S. and Ohtsuka, E. (1988) *Nucleic Acids Res.* **16**, 9443–9456.
24. Bodenhausen, G. and Ruben, D. G. (1980) *Chem. Phys. Lett.* **69**, 185–189.
25. Bax, A., Ikura, M., Kay, L. E., Torchia, D. A. and Tshudin, R. (1990) *J. Magn. Reson.* **86**, 304–318.
26. Yamazaki, T., Yoshida, M., Kanaya, S., Nakamura, H. and Nagayama, K. (1991) *Biochemistry* **30**, 6036–6047.
27. Oda, Y., Yoshida, M. and Kanaya, S. (1993) *J. Biol. Chem.* **268**, 88–92.
28. Morikawa, K. and Katayanagi, K. (1992) *Bull. Inst. Pasteur* **90**, 71–82.
29. Record, M. T., Jr., Lohman, T. M. and De Haseth, P. (1976) *J. Mol. Biol.* **107**, 145–158.
30. Suck, D., Lahm, A. and Oefner, C. (1988) *Nature* **332**, 464–468.
31. McClarin, J. A., Frederick, C. A., Wang, B.-C., Greene, P., Boyer, H. W., Grable, J. and Rosenberg, J. M. (1986) *Science* **234**, 1526–1541.
32. Shindo, H. and Matsumoto, U. (1984) *J. Biol. Chem.* **259**, 8682–8684.
33. Gupta, G., Sarma, M. H. and Sarma, R. H. (1985) *J. Mol. Biol.* **186**, 463–469.
34. Chou, S.-H., Flynn, P. and Reid, B. R. (1989) *Biochemistry* **28**, 2435–2443.
35. Benevides, J. M. and Thomas, G. J. Jr. (1988) *Biochemistry* **27**, 3868–3873.
36. Zimmerman, S. B. and Pfeiffer, B. H. (1981) *Proc. Natl. Acad. Sci. USA* **78**, 78–82.
37. Arnott, S., Chandrasekaran, R., Millane, R. P. and Park, H.-S. (1986) *J. Mol. Biol.* **188**, 631–640.
38. Wang, A. H.-J., Fujii, S., van Boom, J. H., van der Marel, G. A., van Boeckel, S. A. and Rich, A. (1982) *Nature* **299**, 601–604.
39. Salazar, M., Fedoroff, O. Y., Miller, J. M., Ribeiro, S. and Reid, B. R. (1993) *Biochemistry* **32**, 4207–4215.